A Study of the Optimum Design of Wide-Band Parametric Amplifiers and Up-Converters*

GEORGE L. MATTHAEI†, MEMBER, IRE

Summary—Single-diode parametric amplifiers or up-converters using multiple-resonator filters as coupling networks can be made to have considerably larger bandwidths than corresponding amplifiers having single-resonator coupling circuits. Data are presented from which the coupling-filter bandwidths required for given coupling network complexity, diode parameters, and required gain can be determined for both parametric amplifiers and up-converters. In the cases of nondegenerate parametric amplifiers and up-converters, the fact that the diode must be brought to resonance at more than one frequency has an added limiting effect on bandwidth. Some trial amplifier designs are shown, and important considerations in the synthesis of the coupling filters are noted. It is seen that for the case of upper-sideband up-converters, if a filter having n resonators is used in both the input and upper-sideband circuits, then the over-all response can be made to correspond to that of a filter with $2n$ resonators. The gain characteristics of the trial amplifier designs as determined with a digital computer are included. Computed responses ranging in bandwidth from 9 to 27 per cent are obtained for multi-resonator designs having $C_1/C_0=0.25$.

Introduction

IN THE PAST, most single-diode parametric and up-converter amplifiers have been designed with noise figure and gain as the prime consideration, and bandwidth has been of only secondary interest. Except for the paper of Seidel and Herrmann,[1] little attention appears to have been given to the possibility of increasing bandwidth by using coupling networks which are more complex than simple one-resonator tank circuits. In the work described herein, methods of network theory are used in order to predict the performance that can be obtained using coupling networks of any given complexity. In addition, some trial designs are tested by computing their responses with a digital computer.

The nature of the problem of wide-band design can be seen as follows: Suppose that the time variation of a variable-capacitance diode is given by the series[2]

$$C(t) = C_0 + 2C_1 \cos(\omega t + \phi_1) + \cdots . \tag{1}$$

The constant term C_0 represents a fixed, parasitic capacitance which is responsible for the bandwidth limitations of parametric amplifiers and up-converters. Taking the case of parametric amplifiers, the capacitance C_0 may be regarded as an intrinsic part of the input and idler circuits. If, for example, the diode is connected so that C_0 appears as a shunt element at the terminals of the input and idler circuits, then the real part of the impedance $Z(j\omega)$ of each of these circuits is limited as indicated by the integral

$$\int_0^\infty \mathrm{Re} + Z(j\omega)d\omega = \frac{\pi}{2C_0} \tag{2}$$

which is derived by Bode.[3] Since in the operating band of a parametric amplifier it is necessary that the impedances of the input and idler circuits (including C_0) be almost purely real, in view of (2), it is desirable that Re $Z(j\omega)$ go sharply to zero outside of the operating bands of these circuits so that bandwidth capability will not be wasted. Thus to conserve bandwidth capability and to obtain nearly constant gain across the band of interest, it is necessary to use filter structures as input and idler terminating networks.

In the case of nondegenerate parametric amplifiers, *i.e.*, the case where the signal and idler frequency bands do not overlap, two filters are required. In the case of so-called degenerate parametric amplifiers, the signal and idler frequency bands are the same, and one filter suffices for both. The paper of Seidel and Herrmann[1] treated the case of wide-band degenerate amplifiers using the viewpoint of setting derivatives of the gain function equal to zero at midband. The approach herein is quite different and rests directly on filter synthesis techniques.

II. Circuits for Wide-Band Degenerate Amplifiers

From the work of Rowe,[2] it is seen that the operation of a shunt-connected, variable-capacitance diode being pumped at a frequency f_p can be represented by

$$\begin{bmatrix} I_1 \\ I_2^* \end{bmatrix} = \begin{bmatrix} jB_{11} & jB_{12} \\ j(-B_{21}) & j(-B_{22}) \end{bmatrix} \begin{bmatrix} V_1 \\ V_2^* \end{bmatrix} \tag{3}$$

where I_1 and V_1 are, respectively, the current into the diode and the voltage across the diode at the input signal frequency f, and where I_2^* and V_2^* are the conjugates of the analogous current and voltage at the idler frequency

$$f' = (f_p - f). \tag{4}$$

* Received by the PGMTT, July 5, 1960; revised manuscript received, September 15, 1960. This research was supported by the Wright Air Dev. Div., Wright-Patterson AFB, Dayton, Ohio, under Contract AF 33(616)-5803.

† Stanford Res. Inst., Menlo Park, Calif.

[1] H. Seidel and G. F. Herrmann, "Circuit aspects of parametric amplifiers," 1959 WESCON Convention Record, Pt. 2, pp. 83–90.

[2] This definition of C_0 and C_1 is consistent with the work of H. E. Rowe, "Some general properties of nonlinear elements. II. Small signal theory," Proc. IRE, vol. 46, pp. 850–860; May, 1958.

[3] H. W. Bode, "Network Analysis and Feedback Amplifier Design," D. Van Nostrand Co., Inc., New York, N. Y., pp. 280–281; 1945.

The various values of B_{mn} are given by

$$B_{11} = 2\pi f C_0, \qquad B_{12} = 2\pi f C_1$$
$$B_{21} = 2\pi f' C_1, \qquad B_{22} = 2\pi f' C_0. \tag{5}$$

Here, C_0 and C_1 are coefficients of the series in (1), and it is assumed that the diode sees short-circuits at the frequencies corresponding to all other harmonic and sideband frequencies. Examination of (3) to (5) shows that C_0 acts like any other constant, linear capacitance at all frequencies,[4] and that the coupling between signals at frequencies f and f' occurs by way of C_1.

With the above background in mind, let us now examine the degenerate amplifier circuit in Fig. 1. It is shown using a circulator, which will give the largest gain and smallest noise figure; however, a circulator is not necessary as far as design for a given bandwidth is concerned. Neglecting the diode loss resistance for the moment, we see that the diode is represented by C_0 and C_1 in parallel, and C_0 is treated as being incorporated into the first resonator of a band-pass filter circuit. The input admittances Y_b and Y_b' indicated in the figure are the input admittances of this filter at the signal frequency, f, and the idler frequency, f', respectively. They are also the total admittances seen by C_1 at frequencies f and f'. As a result of incorporating C_0 into a filter structure, Y_b and Y_b' are almost purely real over an appreciable frequency band, a condition necessary for wide-band operation. In Fig. 1, the pump signal connections have been omitted for simplicity.

By matrix inversion, the relations of (3) to (5) can be expressed in the form

$$\begin{bmatrix} V_1 \\ V_2^* \end{bmatrix} = \begin{bmatrix} j(-X_{11}) & j(-X_{12}) \\ jX_{21} & jX_{22} \end{bmatrix} \begin{bmatrix} I_1 \\ I_2^* \end{bmatrix}, \tag{6}$$

where

$$X_{11} = \frac{1}{2\pi f C_0(1-a^2)} = \frac{1}{2\pi f C_0^s},$$
$$X_{12} = \frac{a}{2\pi f' C_0(1-a^2)} = \frac{1}{2\pi f' C_1^s}$$
$$X_{21} = \frac{a}{2\pi f C_0(1-a^2)} = \frac{1}{2\pi f C_1^s},$$
$$X_{22} = \frac{1}{2\pi f' C_0(1-a^2)} = \frac{1}{2\pi f' C_0^s} \tag{7}$$

and

$$a = \frac{C_1}{C_0}. \tag{8}$$

The square matrix defined by (6) and (7) gives the corresponding "open-circuit impedances" (for frequencies f and f') for a diode, *having all of its higher harmonics and unwanted sidebands short-circuited.* The approach of Leenov[5] (who dealt with the case of up-converters) would give a somewhat different set of open-circuit impedances because his approach implies that the unwanted harmonics and sidebands are all open-circuited. In a given practical situation, usually, neither representation is entirely accurate, since the various unwanted frequencies usually all see different terminating impedances. For simplicity, the representation in (6) and (7) will be used herein.

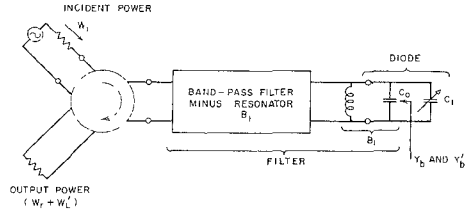

Fig. 1—Degenerate parametric amplifier with variable-capacitance diode resonated in shunt.

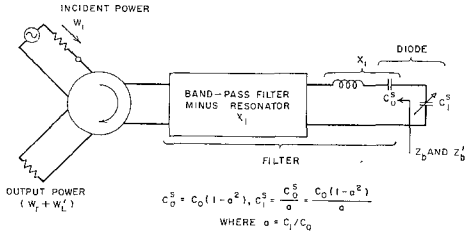

Fig. 2—Degenerate parametric amplifier with variable-capacitance diode resonated in series.

From the open-circuit impedance relations for the diode, we can obtain the series equivalent circuit for the diode as shown in Fig. 2. This representation is convenient when the diode is to become part of a series resonator as shown in this figure. This amplifier with the diode connected in series is essentially the dual of that in Fig. 1, and the same mathematical treatment applies for both. In the discussion to follow the series connection will be emphasized for the following reasons:

1) If the diode is resonated in series, the impedance level required for the associated filter will be lower than if the same diode is resonated in parallel at the same frequency. This makes possible the use of variable capacitance diodes with smaller capacitances which generally have better Q's. It also may make the filter design more convenient.
2) The parasitic series inductance of the diode can be incorporated into the series resonator circuit.
3) Obtaining an $a = C_1/C_0$ ratio which is as large as possible is vital if wide bandwidth is desired. If the diode is resonated in shunt, any stray shunt capacitances add directly to C_0 and decrease the size of the ratio C_1/C_0. It appears probable that when the diode is resonated in series, the deleteri-

[4] Note that in (3), the second equation can also be expressed as $I_2 = jB_{21}V_1^* + jB_{22}V_2$. Thus, for $V_1 = 0$, $I_2/V_2 = jB_{22}$.

[5] D. Leenov, "Gain and noise figure of a variable-capacitance up-converter," *Bell Sys. Tech. J.*, vol. 37, pp. 989–1008; July, 1958.

ous effects of stray capacitance can be minimized, since stray series capacitance should be easier to control.

III. Analysis of Parametric Amplifiers

It will be convenient to redraw the circuits in Fig. 1 as in Fig. 3, and the circuit in Fig. 2 as shown in Fig. 4. Note that in both Figs. 3 and 4 elements G_d or R_s have been added to account for diode losses. Considering the case of Fig. 4, the filter and circulator circuits are seen to have been drawn twice, once for the *signal frequency* f, and once for the *idler frequency* f'. Observe that the impedances evaluated at frequency f' are primed while the impedances evaluated at frequency f are unprimed.

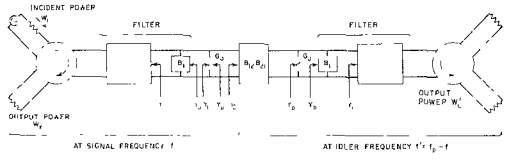

Fig. 3—A parametric amplifier representation which is convenient for purposes of analysis (case of diode resonated in shunt).

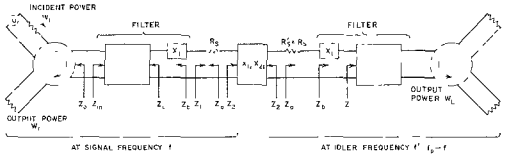

Fig. 4—A parametric amplifier representation which is convenient for purposes of analysis (case of diode resonated in series).

The coupling between the f and f' circuits is represented by the box labeled $X_{12}X_{21}$. Using (6) with $X_{11}=X_{22}=0$ (the reactances X_{11} and X_{22} are removed from the $X_{12}X_{21}$ box and lumped with Z_a and Z_a') and noting that Z_2 in Fig. 4 is E_1/I_1 while Z_a' in the figure would be $-E_2/I_2$, we readily obtain

$$Z_2 = \frac{-X_{12}X_{21}}{Z_a'^*}, \tag{9}$$

where X_{12} and X_{21} are positive quantities given by (7) and $Z_a'^*$ is the complex conjugate of Z_a'. Thus, if Z_a' is real and positive, Z_2 will be real and negative. As a result, this device operates as a negative resistance amplifier. It is also readily shown that Z_a in the figure is related to Z_2' by

$$Z_2' = \frac{-X_{12}X_{21}}{Z_a^*}. \tag{10}$$

In Fig. 4, the incident signal power (*i.e.*, available power) at frequency f is indicated by W_i (following Rowe's notation), while the output power at frequency f is the power W_r which is reflected into the circulator by the filter on the left in Fig. 4. (Of course, as has been mentioned previously, for the case of degenerate amplifiers there is actually only one filter. However, for purposes of analysis we may regard the filter on the right in Fig. 4 as being a second filter operating at frequency f'.) The power gain with respect to W_r is then

$$\frac{W_r}{W_i} = |\Gamma|^2 = \left|\frac{Z_m - Z_0}{Z_m + Z_0}\right|^2, \tag{11}$$

where Γ is the voltage reflection coefficient between the circulator impedance Z_0 and the impedance Z_m seen looking in the left end of the left filter. For our purposes, however, it is much easier to deal with the impedances Z_b and Z_1 rather than Z_0 and Z_m. As is mentioned in Bode,[6] $|\Gamma|$ may be computed by

$$|\Gamma| = \sqrt{\frac{W_r}{W_i}} = \left|\frac{Z_b - Z_1^*}{Z_b + Z_1}\right| \tag{12}$$

where Z_1^* is the complex conjugate of Z_1.[7] Using (9) we then obtain

$$\frac{W_r}{W_i} = \left|\frac{(Z_b - R_s) + \left(\frac{X_{12}X_{21}}{Z_a'^*}\right)^*}{(Z_b + R_s) - \left(\frac{X_{12}X_{21}}{Z_a'^*}\right)}\right|^2. \tag{13}$$

There is also power W_L' at frequency f' given out through the filter on the right in Fig. 4. To compute this we make use of the Manley-Rowe equations,[2] which say in effect that

$$\frac{W_2'}{W_2} = \frac{f'}{f}, \tag{14}$$

where W_2 is defined as the power *into* the box $X_{12}X_{21}$ from the left, and W_2' is defined as the power *into* the box from the right. (In this device W_2 and W_2' are both negative.) The power *into* Z_1 is $W_i - W_r$, so that the power *into* Z_2 is

$$W_2 = (W_i - W_r)\frac{\text{Re } Z_2}{R_s + \text{Re } Z_2}, \tag{15}$$

which is a negative quantity in this case, since $W_i < W_r$, Re $Z_2 < 0$ and in practical cases $R_s < |\text{Re } Z_2|$. By (14), the power $-W_2'$ *out* of the $X_{12}X_{21}$ box is given by (15) times $-f'/f$. The power W_L' is that part of $-W_2'$ which is absorbed in Re Z_b', so that

$$\frac{W_L'}{W_i} = \left(1 - \frac{W_r}{W_i}\right)\frac{\text{Re } Z_2}{R_s + \text{Re } Z_2}\left(\frac{-f'}{f}\right)\frac{\text{Re } Z_b'}{R_s' + \text{Re } Z_b'}, \tag{16}$$

where W_r/W_i is obtained from (13).

[6] Bode, *op. cit.*, p. 364.

[7] For (12) to be valid, it is necessary that the structure between the circulator and the reference plane of Z_b be lossless, or have negligible loss.

If f_0 is the midband frequency for the filter in Fig. 2, then for the degenerate amplifier case it is required that

$$f_0 = f_p/2, \tag{17}$$

where f_p is the pump frequency. Then by (4), if

$$f = f_0 + \Delta \tag{18}$$

$$f' = f_0 - \Delta, \tag{19}$$

and if f is within the pass band of the filters, f' will also be within the pass band of the filter, but at the other side of f_0. As is indicated in Fig. 2, both the "reflected" power, W_r, at frequency f, and the idler power, W_L' at frequency f', will emerge from the output port of the circulator. Since both the outputs at f and f' will carry the modulation, both represent useful power if the amplifier is followed either by a video detector or by another amplifier and then a video detector. Thus, the useful power gain of the device is equal to the sum of the gains given by (13) and (16), which is about 3 db more gain than is given by (13) alone. An exception occurs when f is almost equal to f', so that the difference beat signal between f and f' falls within the pass band of the video amplifier following the crystal video detector. In this case the output power will vary between zero and a peak value of four times that of the signal output power alone, this variation being at a rate corresponding to the difference frequency $|f-f'|$. When $|f-f'|$ exceeds the bandwidth of the video amplifier, this variation is no longer observable. Then the filtering effect of the amplifier averages out the $|f-f'|$ variation so that the video power output is effectively the sum of the signal and idler video outputs (as taken separately).

By duality, equations analogous to (13) and (16) are readily obtained for the shunt diode case in Figs. 1 and 3. They are

$$\frac{W_r}{W_i} = \left| \frac{(Y_b - G_d) + \left(\dfrac{B_{12}B_{21}}{Y_a'^*}\right)^*}{(Y_b + G_d) - \left(\dfrac{B_{12}B_{21}}{Y_a'^*}\right)} \right|^2 \tag{20}$$

and

$$\frac{W_L'}{W_i} = \left(1 - \frac{W_r}{W_i}\right)\frac{\text{Re } Y_2}{G_d + \text{Re } Y_2}\left(\frac{-f'}{f}\right)\frac{\text{Re } Y_b'}{G_d' + \text{Re } Y_b'}. \tag{21}$$

Herein, and for the parametric amplifier and up-converter discussions to follow, the loss elements R_s, R_s', G_d, and G_d' in Figs. 3 and 4 will be defined as:

$$R_s = \frac{1}{Q_d 2\pi f_0 C_0^s} = \frac{(X_{11})_0}{Q_d} \tag{22}$$

$$R_s' = \frac{1}{Q_d' 2\pi f_0' C_0^s} = \frac{(X_{22})_0}{Q_d'} = R_s \tag{23}$$

$$G_d = \frac{2\pi f_0 C_0}{Q_d} = \frac{(B_{11})_0}{Q_d} \tag{24}$$

$$G_d' = \frac{2\pi f_0' C_0}{Q_d'} = \frac{(B_{22})_0}{Q_d'} = G_d\left(\frac{f_0'}{f_0}\right)^2, \tag{25}$$

where f_0 is the center of the signal input band; f_0' is the band center of the idler band (of course, for degenerate amplifiers $f_0 = f_0'$); Q_d is the operating Q of the diode at frequency f_0; $Q_d' = Q_d(f_0/f_0')$ is the operating Q of the diode at frequency f_0'; C_0^s, X_{11}, and X_{22} are given by (7) and (8); and C_0, B_{11}, and B_{22} are given by (5). The brackets and sub zeros are introduced to imply that

$$(X_{11})_0 = X_{11}|_{f=f_0}, \quad (X_{22})_0 = X_{22}|_{f=f_0'}, \text{ etc.} \tag{26}$$

Of course, the equations for R_s and R_s' are based on having the resistor and capacitor in series, while those for G_d and G_d' are based on having the conductance and capacitor in parallel. Computations indicate that the operating Q's, Q_d and Q_d', for typical graded junction diodes may be estimated by

$$Q_d = 0.71\frac{f_c}{f_0} \quad \text{and} \quad Q_d' = 0.71\frac{f_c}{f_0'} \tag{27}$$

where f_c is the usual "cutoff frequency" measured at a bias near the reverse breakdown voltage. These approximate formulas assume that the diode is pumped and biased so that the voltage swings from zero volts to negative voltages closely approaching breakdown.

IV. Band-Pass Filters from Low-Pass Prototypes

Extensive tables of element values now exist for normalized maximally flat and Tchebycheff low-pass filter designs.[8-10] Fig. 5 shows the type of filter treated by these tables and a typical Tchebycheff response. A low-pass filter such as is shown in Fig. 5 is readily converted to an analogous band-pass filter by use of the transformation given in (a) to (c) in Fig. 6. Knowing the generator source impedance, R_g, the fractional bandwidth, w, and the center frequency, f_0, desired for the band-pass filter, we can compute the element values for the band-pass filter from the radian cutoff frequency, Ω_1, and element values of the low-pass prototype (see Fig. 5), by use of (d), (e), and (f) in Fig. 6.

The filter shown in Fig. 6 has lumped elements, but filters for use with parametric amplifiers would probably consist of a mixture of semi-lumped and transmission-line elements. In such cases it is helpful to specify the resonators of a filter in terms of their resonant fre-

[8] L. Weinberg, "Network Design by Use of Modern Synthesis Techniques and Tables," Hughes Aircraft Co., Res. Labs., Culver City, Calif., Tech. Memo. 427; 1956. Also, *Proc. of NEC*, vol. 12; 1956.

[9] L. Weinberg, "Additional Tables for Design of Optimum Ladder Networks," Hughes Aircraft Co., Res. Labs., Culver City, Calif., Tech. Memo. 434; 1956.

[10] W. J. Getsinger, *et al.*, "Research on Design Criteria for Microwave Filters," SRI Project 2326, Contract DA 36-039 SC-74862, Stanford Res. Inst., Menlo Park, Calif. Tech. Rept. 4; December, 1958.

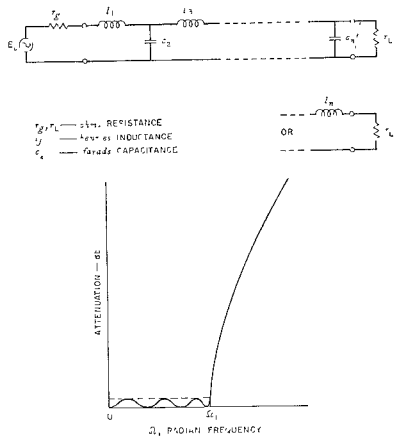

Fig. 5—Low-pass prototype filter and a typical Tchebycheff response.

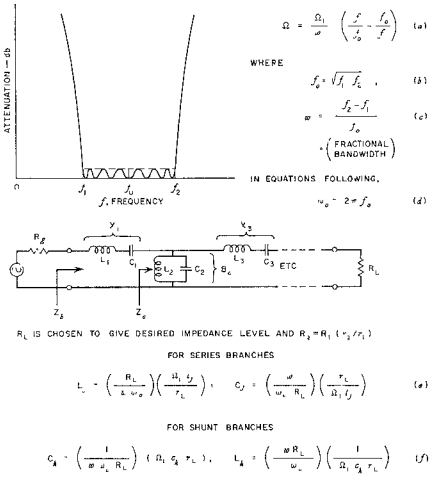

Fig. 6—Summary of relations for design of lumped-element band-pass filters from low-pass prototypes.

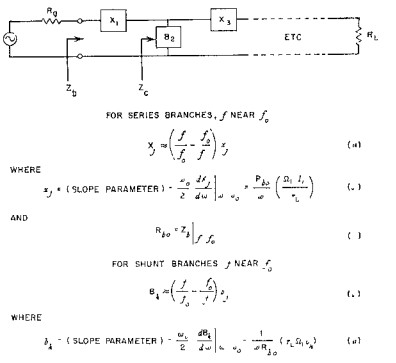

Fig. 7—General description of band-bass filters in terms of resonator slope parameters. (Ω_1, l_j, c_k and r_L are defined in Fig. 5.)

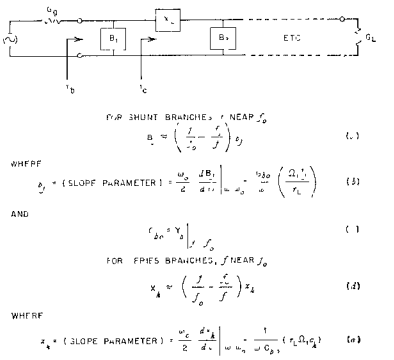

Fig. 8—Slope parameters for dual case to that in Fig. 7. (Ω_1, l_j, c_k, and r_L are defined in Fig. 5.)

quency and their reactance or susceptance slopes, as is done in Fig. 7. Using this description, the exact nature of the resonators is unimportant, except that they must function similarly to series or shunt LC resonators in the vicinity of f_0. As is shown in the figure the parameters l_j, c_k, Ω_1, and r_L from the low-pass prototype, along with R_0, w, and f_0 specified for the band-pass filter can be related directly to resonator *slope parameters* x_j and b_k. From these parameters the required reactance and susceptance slopes are obtained from the equations given. If the resonator boxes in Fig. 7 contain lumped-element resonators, as in Fig. 6, the slope parameters are given by

$$x_j = \overbrace{\frac{1}{\omega_0 C_j}}^{\text{series}} = \omega_0 L_j, \quad \text{and} \quad b_k = \omega_0 C_k = \overbrace{\frac{1}{\omega_0 L_k}}^{\text{shunt}}, \tag{28}$$

where the L's and C's are as defined in Fig. 6. Fig. 8 gives the equations for the circuit which is the dual of that in Fig. 7. If the circuit in Fig. 8 contains lumped-element resonators, then

$$b_j = \overbrace{\omega_0 C_j = \frac{1}{\omega_0 L_j}}^{\text{shunt}}, \quad \text{and} \quad x_k = \overbrace{\omega_0 L_k = \frac{1}{\omega_0 C_k}}^{\text{series}}. \tag{29}$$

V. Gain and Bandwidth Relations for Degenerate Parametric Amplifiers

In the variable-capacitor amplifiers studied on this project, the capacitance C_0 (or C_0^s) of the diode represents a fixed parasitic element which cannot be eliminated. In the degenerate amplifier represented by Figs. 2 and 4, C_0^s is incorporated into the first resonator and by (28) fixes its minimum reactance slope. Thus for Fig. 2 and its representation in the form of Fig. 4, the slope parameters are restricted as follows:

$$x_1 = x_1' \geqq (X_{11})_0 = (X_{22})_0 \tag{30}$$

for the case of degenerate amplifiers which, of course, have $f_0 = f_0'$. The inequality sign in (30) will usually hold as a result of extra reactance slope due to such things as L_1 not being a truly lumped inductance, and reactance effects of the pump circuit coupling. However, for degenerate amplifiers, it should be possible to keep x_1 nearly equal to $(X_{11})_0$.

In order to obtain equations which relate the midband gain of a degenerate amplifier to its filter bandwidth, let us replace the impedances Z_b and Z_b' in Figs. 2 and 4 with the resistance $(Z_b)\big|_{f=f_0} = R_{b0} = R_{b0}'$ defined in (c) of Fig. 7. In Fig. 7, $R_{b0} = R_L$, but the definition in (c) of that figure is used since for some kinds of transmission line filters, R_{b0} will not equal R_L. Then by (13) we can compute

$$|\Gamma_0| = \Gamma_0 = \frac{(R_{b0} - R_s)(R_{b0} + R_s) + (X_{12})_0(X_{21})_0}{(R_{b0} + R_s)(R_{b0} + R_s) - (X_{12})_0(X_{21})_0}, \quad (31)$$

where $|\Gamma_0|^2 = (W_r/W_i)_0$ is the gain near midband *neglecting output due to the idler.* (The idler contributes about 3 db more of useful gain except, possibly, when the signal and idler frequencies are so close that their beat frequency is within the video detector bandwidth.) By (7), (8), and (26), we see that

$$(X_{12})_0 = a(X_{22})_0 \quad \text{and} \quad (X_{21})_0 = a(X_{11})_0. \quad (32)$$

By (31), (32), (22), and (23),

$$\Gamma_0 = \frac{\left(\frac{R_{b0}}{a(X_{11})_0} - \frac{1}{aQ_d}\right)\left(\frac{R_{b0}}{a(X_{11})_0} + \frac{1}{aQ_d}\right) + 1}{\left(\frac{R_{b0}}{a(X_{11})_0} + \frac{1}{aQ_d}\right)^2 - 1}, \quad (33)$$

where the fact that $(X_{11})_0 = (X_{22})_0$ for degenerate amplifiers was also used. Now by (30) it is known that the slope parameter x_1 for the first resonator X_1 will be fixed largely by C_0[8] for the diode. By (b) of Fig. 7,

$$\frac{R_{b0}}{x_1} = w\left(\frac{r_L}{\Omega_1 l_1}\right). \quad (34)$$

Thus, if we know $r_L/(\Omega_1 l_1)$ from the low-pass prototype and have a value for R_{b0}/x_1, we can solve for the fractional bandwidth w. Introducing x_1 in (33) as a cancelling factor we can obtain

$$|\Gamma_0| = \frac{\left(u - \frac{1}{aQ_d}\right)\left(u + \frac{1}{aQ_d}\right) + 1}{\left(u + \frac{1}{aQ_d}\right)^2 - 1}, \quad (35)$$

where

$$u = \frac{R_{b0}x_1}{ax_1(X_{11})_0}. \quad (36)$$

Solving for u, and then for w by use of (34) gives the filter fractional bandwidth

$$w = a\left(\frac{(X_{11})_0}{x_1}\right)\left(\frac{\Omega_1 l_1}{r_L}\right)\left[\sqrt{\left[\frac{1}{2aQ_d}\left(\frac{\Gamma_0+1}{\Gamma_0-1}+1\right)\right]^2 - \left(\frac{\Gamma_0+1}{\Gamma_0-1}\right)\left(\frac{1}{(aQ_d)^2}-1\right)} - \left[\frac{1}{2aQ_d}\left(\frac{\Gamma_0+1}{\Gamma_0-1}+1\right)\right]\right]. \quad (37)$$

If Q_d is very large, then (37) reduces to

$$w = a\left(\frac{(X_{11})_0}{x_1}\right)\left(\frac{\Omega_1 l_1}{r_L}\right)\sqrt{\frac{\Gamma_0+1}{\Gamma_0-1}}, \quad (38)$$

which is a convenient form for examining the significance of the various parameters. Note that w is directly proportional to $a = C_1/C_0$ so that it is of great importance that the diode be pumped as hard as is allowable, if maximum bandwidth is desired. If the gain is low so that Γ_0 is not much greater than one, then w is a strong function of gain. However, as the gain becomes larger, the quantity under the radical approaches one and the bandwidth becomes a very weak function of gain. Thus, it is seen that the gain-bandwidth product will not be constant as the gain is varied if the lumped-element prototype parameter $\Omega_1 l_1/r_L$ remains fixed. Lombardo and Sard[11] report a gain-bandwidth product which is constant as the gain is varied, for the case of amplifiers with single-resonator filters. In their case the bandwidth is defined as the 3-db points and this bandwidth will decrease as the gain is increased for a single-resonator design. The analogous multiple-resonator Tchebycheff design situation is to vary the prototype (and hence, $\Omega_1 l_1/r_L$) as the gain is varied so that the ripples of gain will always have the same db amplitude no matter what the average gain is. On that basis, something approaching a constant gain-bandwidth product vs gain may also result for multiple-resonator designs. However, if the prototype used remains fixed for a series of designs, having progressively increasing midband gains, the tendency will be for the size of the gain ripples to increase for designs with larger midband gains, while the equal-ripple bandwidth will change very little once gains of around 20 db or so are reached.

In order to facilitate the use of (37), the chart in Fig. 9 was computed. Using this chart, if a given gain in the vicinity of midband is desired (note that the abscissa is gain with respect to output at the signal frequency only), then knowing (aQ_d) for the diode to be used, the parameter h can be determined from the ordinate. If the diode is to be resonated in series, then the fractional bandwidth parameter for the filter can be computed by

$$w = ha\left(\frac{(X_{11})_0}{x_1}\right)\left(\frac{\Omega_1 l_1}{r_L}\right). \quad (39)$$

[11] P. P. Lombardo and E. W. Sard, "Low-noise microwave reactance amplifiers with large gain-bandwidth products," 1959 WESCON Convention Record, Pt. 1, pp. 83–98.

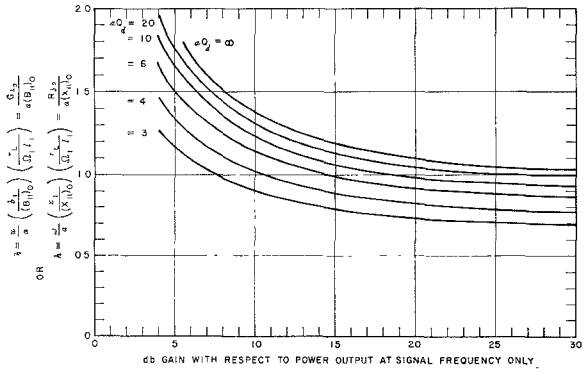

Fig. 9—Chart for relating degenerate parametric amplifier gain and filter bandwidth for a given low-pass prototype and for given diode parameters. (The idler contributes about 3 db additional gain to the gain indicated on the abscissa of this chart.)

If the diode is to be resonated in shunt, then the analogous relation

$$w = ha\left(\frac{(B_{11})_0}{b_1}\right)\left(\frac{\Omega_1 l_1}{r_L}\right) \tag{40}$$

applies.

From (39) and (40) it is seen that w depends strongly on $(\Omega_1 l_1/r_L)$ obtained from the lumped-element prototype. In order to obtain large fractional bandwidths, w, it is desirable that $(\Omega_1 l_1/r_L)$ be large. However, it will be found that prototype filters which will lead to amplifiers with more nearly constant gain throughout their operating band will tend to have smaller values of $(\Omega_1 l_1/r_L)$, and hence, somewhat smaller bandwidths. Thus the choice of the lumped-element prototype involves a compromise between the objective of obtaining wide bandwidth and the objective of obtaining nearly constant gain. It should also be recognized that adding additional elements to the filter will also improve the performance. This is because additional elements facilitate holding the gain close to a desired value throughout the pass band, and they also permit a sharper cutoff, which improves the bandwidth capabilities, as was discussed with reference to (2).

If Ω_1 is the equal-ripple band edge of an ordinary low-pass Tchebycheff filter with resistor terminations, the fractional bandwidth w obtained with the aid of Fig. 9 and (39) or (40) will be the bandwidth of the corresponding band-pass filter for the amplifier *when connected to resistor terminations corresponding to those of the prototype.* As will be seen from the examples to follow, the negative-resistance type of termination presented by a pumped, variable-capacitance diode affects the response shape and bandwidth in a different way than does an ordinary resistor and, as a result, the actual operating bandwidth of the amplifier is somewhat larger than would be indicated by w. For w to predict the bandwidth of the amplifier with high accuracy, Ω_1 must be the band-edge frequency of the low-pass prototype when operated into a termination analogous to a pumped, variable-capacitance diode.

VI. Some Degenerate Parametric Amplifier Examples

Fig. 10 shows a degenerate amplifier configuration having two resonators. The pump circuit is assumed to be so loosely coupled as to have negligible effect at frequencies away from the pump frequency, f_p. Design No. 1 listed in the figure was obtained using an $n=2$ reactive-element, lumped-element prototype having 0.01-db Tchebycheff ripple.[10] The prototype elements as defined in Fig. 5 are $r_g=1$, $l_1=0.4488$, $c_2=0.4077$, $r_L=1.1008$, and $\Omega_1=1$. If we hypothesize a diode having a cutoff frequency of $f_c=85$ kMc, and if $f_0=f_0'=1$ kMc then, by (27), $Q_d=Q_d'=60$. Let us assume that $a=C_1/C_0=0.25$, and that we desire about 15.5-db total gain near midband (including output at both the signal and idler frequencies). To obtain 15.5-db total gain near midband, we need 12.5-db gain near midband for the output at the signal frequency alone. For 12.5-db gain and $(aQ_d)=0.25\ (60)=15$, it is seen that $h=1.17$. If we assume that $x_1/(X_{11})_0\approx 1$, then (39) calls for a fractional bandwidth $w=0.121$ for the 0.1-db equal-ripple band of the filter (when connected to resistor terminations). Then by (b) and (e) of Fig. 7, the slope parameters for the two resonators are computed to be $x_1=3.70$ and $b_2=3.36$, taking $R_{b0}=r_L=1.1008$.

Fig. 11 shows the computed input impedance, Z_b, for Design 1, and Fig. 12 shows its computed gain. Note that the equal-ripple band edges for the filter operated with normal resistor terminations extend from about $f/f_0=0.94$ to $f/f_0=1.06$, corresponding to $w=0.121$, but these band-edge points have turned out to be points of peak gain when this filter is used in the variable-capacitance amplifier of Fig. 10. The reason for this will be clear by examination of Fig. 11 and (13). If $Z_a'=Z_b+R_s=R$ and $R=\sqrt{X_{12}X_{21}}$, then the gain will be infinite and oscillation will result. When Re $Z_b=R_b$ in Fig. 11 crosses $\sqrt{X_{12}X_{21}}$, oscillation is prevented by the fact that Im $Z_b=X_b$ is not zero. Clearly, in order to lower the gain peaks in Fig. 12 it will be necessary to increase the input reactance at the points where $R_b=\sqrt{X_{12}X_{21}}$. This tendency for the gain to rise as Re Z_b starts to fall causes the bandwidth to tend to be larger for a degenerate parametric amplifier using a given filter than the bandwidth would be for the same filter operated in a passive circuit with normal resistive terminations.

The desired extra input reactance characteristic was obtained in Design No. 2 by reducing the slope parameter for the second resonator to $b_2=2.35$, while keeping the diode and Resonator 1 as they were previously. The resulting input impedance and gain is shown by the heavy lines in Figs. 11 and 12. As can be seen from the gain plot, the pass-band ripple has been reduced to about 1.6 db.

Using $b_2=0$, and x_1 and the diode as before, a single-resonator design was obtained (Design No. 3). The response of this design is also plotted in Fig. 12. Note that

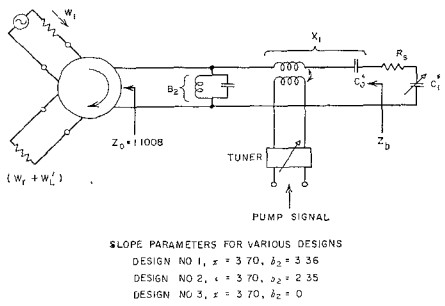

Fig. 10—Circuit for degenerate parametric amplifier examples using a two-resonator filter.

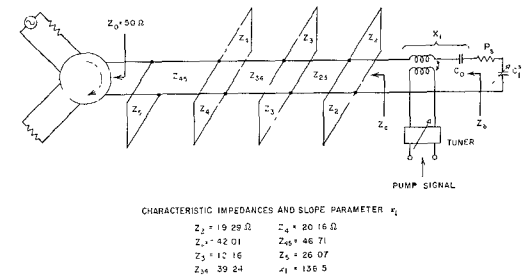

Fig. 13—A five-resonator, degenerate, parametric amplifier design example.

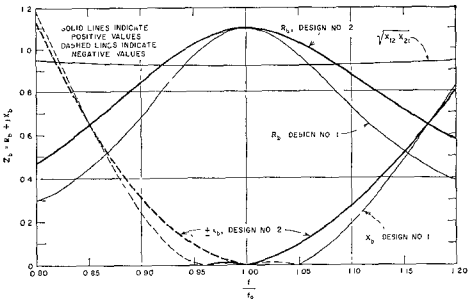

Fig. 11—Computed input impedance, Z_b, for Designs Nos. 1 and 2 in Fig. 10.

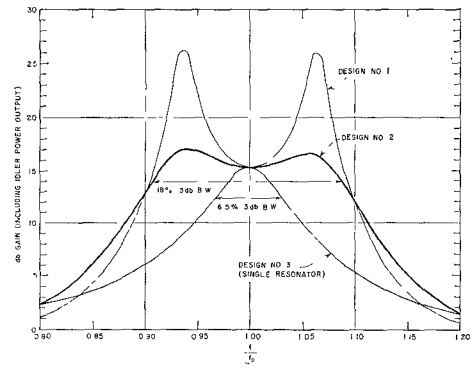

Fig. 12—Computed gain for Designs Nos. 1, 2, and 3 in Fig. 10 using a diode having $a = C_1/C_0 = 0.25$ and $Q_d = 60$.

increasing the number of resonators from one to two makes possible an increase in 3-db bandwidth from 6.5 per cent to 18 per cent. Adding additional resonators can increase the potential bandwidth even further, but the amount of improvement per additional resonator will decrease rapidly as the number of resonators is increased.

Fig. 13 shows another design using a five-resonator filter. The transmission-line portion of the filter was designed using a 0.10-db Tchebycheff-ripple, four-reactive-element prototype having an infinite impedance current generator at one end.[9] If the current of the generator is I_g, then the power delivered into the filter (and to the load resistor at its other end) is

$$P = |I_g|^2 \operatorname{Re} Z_b \qquad (41)$$

where Z_b is the input impedance of the filter. It is thus seen that for a Tchebycheff filter of this type, the real part of the input impedance will be a Tchebycheff approximation of a constant value in the pass band. Since a nearly constant Re Z_b is desirable to obtain a constant gain, this type of prototype appears to be useful for parametric amplifier design. The four-resonator transmission line portion of the filter was designed from the prototype[12] using microwave filter design techniques developed at this laboratory[13,14] As is seen from the $R_c/Z_0 = Z_b/Z_0$ curve in Fig. 14, it has a very nearly Tchebycheff approximation to a constant Re Z_b throughout the pass band. As is shown by the X_c/Z_0 curves, the input impedance of the transmission line filter has an excessive amount of imaginary part. The slope parameter x_1 of the resonator X_1 was chosen so as to largely cancel this imaginary part while leaving a sizable reactance at the points where Re $Z_b = \sqrt{X_{12}X_{21}}$, and it was assumed again that $a = C_1/C_0 = 0.25$. Since the impedance function, Z_c, for the transmission-line portion of the filter has arithmetic symmetry, while the reactance of the diode resonator, X_1, does not, resonator X_1 was tuned about one per cent low so that the total net reactances in the vicinity of cutoff on both sides will be of nearly equal amplitude.

Using $a = 0.25$ and $Q_d = 60$, as for Designs Nos. 1 to 3, the gain was computed and plotted in Fig. 15. In this case the design gain is lower (roughly 10 db including signal and idler power). Since the gain of high-gain parametric amplifiers is a hypersensitive function of their input impedance, in the case of wide-band parametric amplifiers it may be necessary to use lower gains so that the adjustments will not be so critical. If the parametric amplifier is being used simply as a relatively

[12] In this case the slope parameters of the shunt transmission line resonators cannot be obtained from the prototype by the relations in Figs. 7 or 8, as a result of the selectivity effects of the connecting lines. However, it would be possible to relate Resonator 1 to a prototype as is done in Fig. 7, since X_1 has no $\lambda_0/4$ connecting line.

[13] G. L. Matthaei and P. S. Carter, Jr., "Design Criteria for Microwave Filters and Coupling Structures," Tech. Rept. 7, SRI Project 2326, Contract DA 36-039 SC-74862, Stanford Res. Inst., Menlo Park, Calif.; July, 1959.

[14] G. L. Matthaei, "Band-pass microwave filter design—a new method and its relation to other methods," 1960 IRE National Convention Record, pt. 3, pp. 95–122.

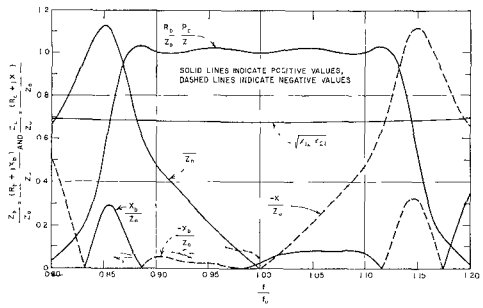

Fig. 14—Computed input impedances Z_b and Z_c for the circuit in Fig. 13.

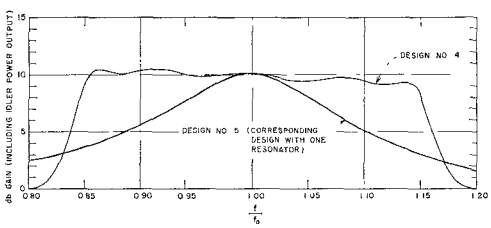

Fig. 15—Computed gain for the amplifier in Fig. 13 and also for an analogous one-resonator amplifier both using a diode having $a=C_1/C_0=0.25$ and $Q_d=60$.

low-noise first-stage amplifier, then gains as low as 10 db may be acceptable in many cases. Of course, lower gain also gives larger bandwidth. Note that in this case the gain is very flat, with only about 0.5-db ripple. If the design had been carried out to give larger gain ripples, a larger minimum gain could probably have been obtained for the same bandwidth. Observe that the gain has a slight slope to it throughout the operating band. This is due to the f'/f factor in (16). The bandwidth of the equal-ripple portion of the response is seen to be about 29 per cent in this case.[15]

Note that in Fig. 13 it would have also been possible to resonate the diode in shunt and use a $\lambda_0/4$ line between the diode resonator and shunt stubs Z_2. Besides other possible disadvantages of resonating the diode in shunt, such a scheme would yield a smaller operating bandwidth because of the selectivity of the $\lambda_0/4$ line between resonators 1 and 2. As a result of this extra selectivity, the slope parameter of the diode resonator would have to be less for a given bandwidth or, putting it another way, the bandwidth would have to be less for a given slope parameter. As a result, it is advantageous to have the first resonator in series and the second one in shunt, or vice versa, so that $\lambda_0/4$ coupling lines are not required adjacent to the diode resonator.

VII. Choice of Lumped-Element Prototypes for Amplifier Filters

As can be seen from the preceding examples, the requirements on filters for parametric amplifiers are somewhat different than for filters used in more conventional applications. Assuming that the diode is being resonated in series, for a given db ripple in gain, the real part of the input impedance must be much more nearly constant for a parametric amplifier filter than for a conventional filter. It is also very important that there be a sizable reactive component when Re Z_b starts to fall at the band edge.

The input impedances of several common types of filters were computed to investigate their usefulness for amplifier applications. Conventional Tchebycheff filters having resistive terminations at both ends were found to have the characteristic that Re Z_b ranges above the generator resistance value, R_g, for frequencies near $\Omega=0$, but ranges below the R_g value at frequencies approaching cutoff. In this respect, Re Z_b for a prototype having an infinite impedance generator (as discussed with respect to Design No. 4) is different, since for that type of prototype Re Z_b has equal ripples about a constant value. A maximally flat filter design having resistive terminations at both ends had a relatively small reactive component at frequencies where Re Z_b was falling. As previously noted, this is undesirable.

Further investigation is desirable to determine general methods for obtaining optimum filter designs for parametric amplifiers. Working back from Design No. 2, we obtain the prototype elements $r_g=1$, $l_1=0.592$, $c_2=0.376$, $r_L=1.1008$, $\Omega_1=1$ where in this case Ω_1 is the low-pass prototype radian frequency corresponding to equal-ripple band-edge points in the response of Design No. 2 in Fig. 12. It is seen that these prototype element values differ significantly from those of the 0.01-db ripple, two-reactive-element prototype used for Design No. 1. Although Design No. 4 has a very flat response, a design from a somewhat different prototype could probably have given a little more bandwidth for the same gain and gain ripple (or more gain for the same bandwidth and gain ripple).

VIII. Nondegenerate Parametric Amplifiers

Fig. 16 shows a circuit for a nondegenerate parametric amplifier analogous to the degenerate amplifier in Fig. 10. In this case f_0, the center of the signal band, and f_0', the center of the idler band, are widely separated and two filters are required in order to obtain the proper performance. In Fig. 16, the resonator B_2 belongs to the signal filter which is terminated by the circulator. The resonator B_2' belongs to the idler filter, while R_L' provides the idler termination. The series branch in this circuit contains the diode which introduces the parameters C_0^s, C_1^s, R_s as previously discussed, and in this case the parasitic series inductance L_d of the diode is also shown. The diode is brought to series resonance at *both* f_0 and f_0' by introduction of a length of series transmission line short-circuited at the end. Thus, the series branch in Fig. 16 operates as resonator X_1 for the signal filter at frequencies near f_0, while it operates as resonator X_1' for the idler filter at frequencies near f_0'. Using

[15] The transmission line filter was designed for 25 per cent equal-ripple bandwidth when driven by a current generator.

a semistripline construction, the series transmission line stub might be realized to a satisfactory approximation as fine wire transmission line between the ground plates.

The circuit in Fig. 16 can also be represented as in Fig. 4, but care must be used in relating the two forms. Branch X_1+R_s in Fig. 4 should contain the impedance of the entire circuit to the right of resonator B_2 in Fig. 16 (except for C_1^s) measured at the signal frequency f. Meanwhile, the branch $R_s'+X_1'$ in Fig. 4 should contain the impedance of the entire circuit to the left of resonator B_2' in Fig. 16 (again, except for C_1^s) measured at the idler frequency $f'=f_p-f$. Since the impedance of B_2' is very low at the signal frequency f, while the impedance of B_2 is very low at the idler frequency f', the impedances X_1+R_s and $R_s'+X_1'$ in Fig. 4 are, for most practical purposes, the impedances of the series arm in Fig. 16 (minus C_1^s) at frequencies f and f', respectively. For the case of nondegenerate amplifiers, the circulator on the right in Fig. 4 should, of course, be replaced by a load resistor.

Fig. 17 shows a typical reactance characteristic such as might result from the C_0^s, L_d, and series line combination in Fig. 16. Frequency f_{01} is defined as the resonant frequency of resonator X_1, while f_{01}' is the resonant frequency of resonator X_1'. At frequency f_{01} the series line would usually look inductive, while at f_{01}' it may look either capactive or inductive depending on the relative sizes of C_0^s and L_d. The line is $\lambda/4$ long at frequency f_R, and hence causes infinite reactance at that frequency, while the line would be close to $\lambda/2$ long at frequency f_{01}'.

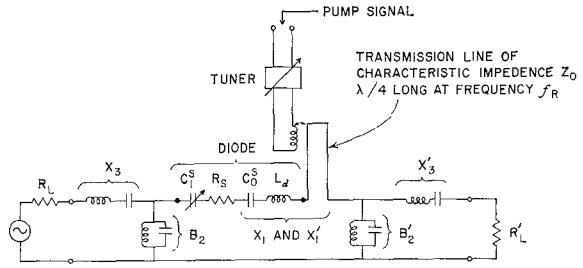

Fig. 16—Example of a nondegenerate parametric amplifier using a two-resonator filter in the signal circuit and also in the idler circuit.

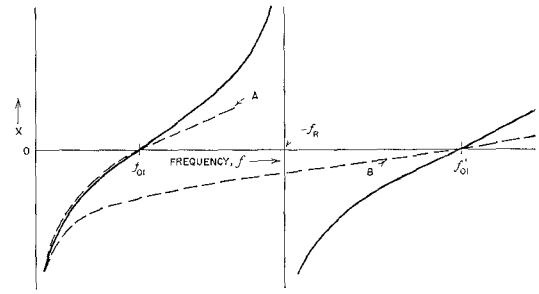

Fig. 17—An approximate reactance curve for the resonator circuit formed by C_0^s, L_d and the transmission line in Fig. 16.

Some previous writers have assumed, in effect, that the diode capacitance C_0^s (or C_0 for the shunt case) can be resonated out independently at the frequencies f_{01} and f_{01}'. If that were possible, the reactance curve for resonator X_1 in Fig. 4 would be approximately as shown by the dashed curve marked A in Fig. 17, while the reactance curve for resonator X_1' would be as shown by the dashed curve marked B. (Each of the curves corresponds approximately to C_0^s in series with a lumped inductance.) Curves A and B would yield considerably smaller reactance slope in the vicinity of f_{01} and f_{01}', and hence, would yield greater bandwidth than would the solid, multiple resonance curve in Fig. 17. However, since resonators X_1 and X_1' must both contain the same element C_0^s, their circuitry is necessarily interconnected and there appears to be no way of avoiding the use of multiple resonances in the reactance curve for resonators X_1 and X_1'. This extra reactance slope which occurs in the nondegenerate amplifier case increases the slope parameters x_1 and x_1' and tends to reduce the bandwidth possible as compared with a corresponding degenerate amplifier.

For maximum amplifier bandwidth the signal and idler filters should have the same bandwidth. If w is the signal filter fractional bandwidth while w' is the idler filter fractional bandwidth, then we require that

$$\frac{w'}{w} = \frac{f_0}{f_0'}. \tag{42}$$

Assuming that both the signal and idler filters are to be designed from the same lumped-element prototype, we may use (b) in Fig. 7 to derive the equation:

$$\frac{x_1}{R_{b0}} = \frac{x_1'}{R_{b0}'}\left(\frac{f_0}{f_0'}\right), \tag{43}$$

or

$$R_{b0}' = (R_{b0})\left(\frac{f_0}{f_0'}\right)\left(\frac{x_1'}{x_1}\right). \tag{44}$$

If the diode is resonated in shunt, the analogous relation

$$G_{b0}' = (G_{b0})\left(\frac{f_0}{f_0'}\right)\left(\frac{b_1'}{b_1}\right) \tag{45}$$

applies. Using Fig. 4 as a model, by use of (13) we may relate the design bandwidth of the filters to the midband gain for given x_1, x_1', a, Q_d and filter prototype parameters. Using (13) and (43) and the fact that

$$(X_{12})_0 = a(X_{22})_0 = a(X_{11})_0\left(\frac{f_0}{f_0'}\right), \tag{46}$$

$$(X_{21})_0 = a(X_{11})_0, \tag{47}$$

and

$$Q_d' = Q_d\left(\frac{f_0}{f_0'}\right), \tag{48}$$

we obtain after considerable manipulation

$$u = \sqrt{\left[\frac{1}{2q}\left(\frac{\Gamma_0+1}{\Gamma_0-1}+\gamma\right)\right]^2+\frac{\Gamma_0+1}{\Gamma_0-1}\left(1-\frac{\gamma}{q^2}\right)} - \left[\frac{1}{2q}\left(\frac{\Gamma_0+1}{\Gamma_0-1}+\gamma\right)\right] \quad (49)$$

where

$$\Gamma_0 = \sqrt{\frac{W_r}{W_i}}\bigg|_{f=f_0} \quad (50)$$

$$\gamma = \frac{f_0'}{f_0}\frac{x_1}{x_1'} \quad (51)$$

$$q = aQ_d\sqrt{\frac{x_1}{x_1'}} \quad (52)$$

$$u = \frac{R_{b0}}{ax_1}\frac{\sqrt{x_1x_1'}}{(X_{11})_0} = \frac{w}{a}\left(\frac{r_L}{\Omega_1 l_1}\right)\frac{\sqrt{x_1x_1'}}{(X_{11})_0}. \quad (53)$$

If the diode is resonated in shunt, (49) and (50) still apply but

$$\gamma = \left(\frac{f_0'}{f_0}\right)^3\left(\frac{b_1}{b_1'}\right) \quad (54)$$

$$q = aQ_d\sqrt{\frac{b_1}{b_1'}}\left(\frac{f_0'}{f_0}\right) \quad (55)$$

and

$$u = \frac{G_{b0}}{ab_1}\frac{\sqrt{b_1b_1'}}{(B_{11})_0}\frac{f_0}{f_0'} = \frac{w}{a}\left(\frac{r_L}{\Omega_1 l_1}\right)\frac{\sqrt{b_1b_1'}}{(B_{11})_0}\frac{f_0}{f_0'}. \quad (56)$$

Using (49), charts were prepared of u vs γ for various values of q and Γ_0. Figs. 18(a), (b), and (c) show such charts for the cases of $\Gamma_0=3.162$ (10-db gain); $\Gamma_0=5.623$ (15-db gain); and $\Gamma_0=10$ (20-db gain), respectively. To use these charts (for the series resonance case) one first designs the diode circuitry to give the resonances for X_1 and X_1' so that x_1 and x_1' can be computed. Then knowing a, Q_d, and f_0'/f_0, γ and q are determined by (51) and (52). From the chart for the desired gain we obtain u, and then by (53) the fractional bandwidth of the input filter must be

$$w = ua\left(\frac{(X_{11})_0}{\sqrt{x_1x_1'}}\right)\left(\frac{\Omega_1 l_1}{r_L}\right). \quad (57)$$

If the diode is resonated in shunt the corresponding equation is

$$w = ua\left(\frac{f_0'(B_{11})_0}{f_0\sqrt{b_1b_1'}}\right)\left(\frac{\Omega_1 l_1}{r_L}\right). \quad (58)$$

Note that in the nondegenerate parametric amplifier case it is important to keep $\sqrt{x_1x_1'}$ (or $f_0/f_0'\sqrt{b_1b_1'}$) as small as possible if the bandwidth is to be maximized.

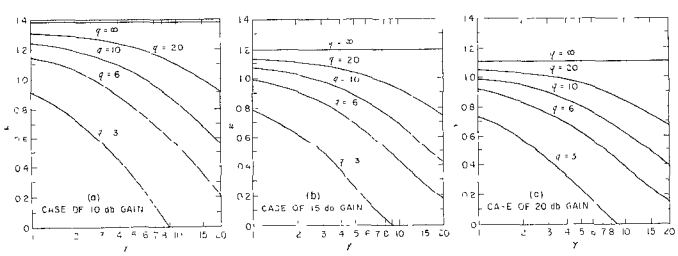

Fig. 18—Charts for determining the filter bandwidths of nondegenerate parametric amplifiers. [The definition and use of quantities u, γ, and q will be found in (49) to (58) and the accompanying discussion.]

IX. Nondegenerate Parametric Amplifier Examples

A normalized design example was worked out on the basis of the circuit in Fig. 16. To facilitate comparison with the degenerate amplifier Design No. 2 (where $x_1=(X_{11})_0=3.70$), in this case $(X_{11})_0$ was also chosen as 3.70. Taking $f_0=500$ Mc and $f_0'=2500$ Mc we have $f_0'/f_0=5$. For simplicity it was assumed that the diode's internal inductance L_d causes the diode to be self-resonant at 2500 Mc. This, then, calls for $(X_L)_0=3.70/(5)^2=0.148$, where $(X_L)_0$ is the reactance of L_d at frequency f_0. Since the diode is self-resonant at frequency f_0', the series line in Fig. 16 is chosen to be $\lambda/2$ long at frequency f_0', so as to also be resonant. This gives $f_R/f_0=2.5$, where f_R was defined in Fig. 17. (Note that here we have taken $f_{01}=f_0$ and $f_{01}'=f_0'$.) Then to bring the diode to resonance at frequency f_0 it is required that the series line have a normalized characteristic impedance of $Z_0=4.90$. Having thus defined the series reactance branch in Fig. 16, the resonator slope parameters x_1 and x_1' were computed to be 4.27 and 8.42, respectively, by use of (b) in Fig. 7. Note that these values are considerably larger than the values $x_1=(X_{11})_0=3.70$ and $x_1'=(X_{22})_0=0.740$ which they could assume if it were possible to resonate the diode at the two frequencies f_0 and f_0' independently.

The diodes for Designs Nos. 1, 2, and 3 were taken to have $a=C_1/C_0=0.25$, with $Q_d=60$ for $f_0=1000$ Mc. In this case $a=0.25$ was used with $Q_d=120$, corresponding to an identical diode operated with $f_0=500$ Mc. The lumped-element prototype values used were the values $r_g=1$, $l_1=0.592$, $c_2=0.376$, $r_L=1.1008$, and $\Omega_1=1$ discussed in Section VII. Using Fig. 18(b) and (57), the signal filter fractional bandwidth for 15-db gain was found to be $w=0.091$. By (b) of Fig. 7

$$R_{b0} = wx_1\left(\frac{r_L}{\Omega_1 l_1}\right) \quad (59)$$

was obtained for the computation of R_{b0}, and R_{b0}' was computed by use of (44). Slope parameters b_2 and b_2' were obtained by (e) in Fig. 7,[16] and the entire design is tabulated in Table I under Design No. 6.

[16] Note that w' from (42) and R_{b0}' must be used in computing b_2'.

TABLE I

NORMALIZED DESIGN PARAMETERS FOR DESIGNS NOS. 6, 7, AND 8
(Nondegenerate Parametric Amplifiers of Form in Fig. 16)

Design No. 6	
Frequencies:	
$f_0'/f_0=5,$	$f_p/f_0=6$
For Diode:	
$(X_{11})_0=3.700,$	$a=C_1/C_0=0.25$
$(X_L)_0=0.1480,$	$Q_d=120$
For Series Transmission Line:	
$Z_0=4.889,$	$f_R/f_0=2.5$
Resonator Slope Parameters and Other Filter Parameters:	
$x_1=4.271,$	$b_2=6.282$
$x_1'=8.420,$	$b_2'=79.66$
$f_{01}/f_0=1,$	$f_{02}/f_0=1$
$f_{01}'/f_0=5,$	$f_{02}'/f_0=5$
(where f_{01}, f_{02}, f_{01}' and f_{02}' are the resonant frequencies of resonators X_1, B_2, X_1', and B_2', respectively)	
$R_{b0}=R_L=0.7233,$	$R_{b0}'=R_L'=0.2852$
Design No. 7	
Same as Design No. 6 except that:	
$f_{02}/f_0=0.9970,$	$f_{02}'/f_0=5.0006$
$f_p/f_0=5.9976$	
Design No. 8	
Same as Design No. 6 except that:	
$b_2=b_2'=0$	
to give single-resonator filters.	

The dashed line in Fig. 19 shows the response of Design No. 6 as computed with a digital computer by methods based on (13). Its midband gain is nearly 15 db, as expected, while its 3-db bandwidth is about 9 per cent. This is somewhat less than anticipated since, as mentioned in Section VII, Ω_1 for the prototype was derived from the equal-ripple band edge for Design No. 2. Thus an equal-ripple bandwidth of about 9 per cent was at first expected. The difference between the anticipated and computed results is probably related to the fact that Design No. 2 was operating with about 12.5 midband gain with respect to the signal frequency, while this design is operating with 15-db gain midband gain with respect to the signal frequency. This corresponds to the $\sqrt{X_{12}X_{21}}$ line in Fig. 11 crossing the R_b curve at a higher level in this latter case, which would tend to narrow the bandwidth.

Due to the relatively large slope of $\sqrt{X_{12}X_{21}}$ vs frequency for nondegenerate amplifiers, the response for Design No. 6 tilts down towards higher frequencies. Design No. 7 listed in Table I has the No. 2 resonators of the filters detuned slightly to compensate for this. The results are as indicated by the heavy solid curve in Fig. 19. Design No. 8 has the slope parameters b_2 and b_2' set to zero to give a design with single resonators.[17]

[17] Of course for a practical circuit with single resonators some means would have to be provided to short out R_L' at signal frequencies f, and R_L at idler frequencies f'.

As with the degenerate amplifier case in Fig. 12, use of two-resonator filters gives slightly over three times the bandwidth which would result if single resonator filters were used. Observe that the fractional bandwidth achieved with the degenerate amplifier is twice that achieved with the nondegenerate amplifier, mostly as a result of the relatively large values of x_1 and x_1' in the latter case.

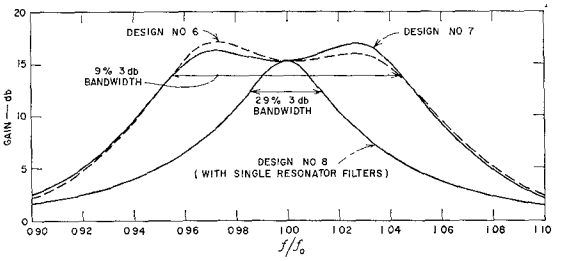

Fig. 19—Computed responses of some trial nondegenerate parametric amplifier designs of the form in Fig. 16 using the parameters listed in Table I.

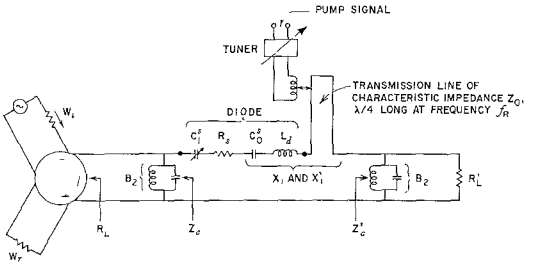

Fig. 20—Up-converter circuit having three input resonators and three upper-sideband resonators.

X. THEORY OF WIDE-BAND UP-CONVERTERS

Fig. 20 shows an up-converter circuit using circuitry similar to that in Fig. 16. In this case the lower-sideband frequency (f_p-f) is suppressed and the primed resonators comprise a filter which passes *upper-sideband* frequencies f', where in this case f' is defined as

$$f'=f_p+f. \tag{60}$$

The circuit can again be analyzed in the form in Fig. 4 (the circulators, of course, are not needed since the output and input are at separate ports). In this case, however, it can easily be shown from Rowe's work[2] [in a manner similar to the derivation of (9) and (10)] that if f' is defined by (60) then

$$Z_2=\frac{X_{12}X_{21}}{Z_a'} \tag{61}$$

and

$$Z_2'=\frac{X_{12}X_{21}}{Z_a} \tag{62}$$

apply instead of (9) and (10). According to the Manley Rowe equations,[2] (14) becomes for this case

$$\frac{W_2'}{W_2} = -\frac{f'}{f} \quad \text{or} \quad \frac{-W_2'}{W_2} = \frac{f'}{f}, \tag{63}$$

which implies that whatever power enters the left side of the $X_{12}X_{21}$ box in Fig. 4 will be emitted from the right side of the box amplified by the ratio f'/f. In a manner paralleling (12) to (16), we obtain for this case

$$\frac{Wr}{Wi} = \left| \frac{(Z_b - R_s) - \left(\frac{X_{12}X_{21}}{Z_a'}\right)^*}{(Z_b + R_s) + \left(\frac{X_{12}X_{21}}{Z_a'}\right)} \right|^2 \tag{64}$$

and

$$\frac{W_L'}{W_i} = \left(1 - \frac{W_r}{W_i}\right) \frac{\text{Re } Z_2}{R_s + \text{Re } Z_2} \left(\frac{f'}{f}\right) \frac{\text{Re } Z_b'}{R_s' + \text{Re } Z_b'} \cdot \tag{65}$$

It can be shown that at midband the gain becomes

$$\left(\frac{W_L'}{W_i}\right)_0 = \left(\frac{f_0'}{f_0}\right) \frac{4R_{b0}R_{b0}'(X_{12}X_{21})_0}{[(R_{b0} + R_s)(R_{b0}' + R_s') + (X_{12}X_{21})_0]^2} \tag{66}$$

where, as before, the subzeros are used to indicate that the various quantities are to be evaluated at frequencies f_0 or f_0' as is appropriate. Corresponding equations for the case where the diode is resonated in shunt are easily obtained by duality.

Eqs. (61) and (62) indicate that when f' is the upper-sideband frequency given by (60), then the $X_{12}X_{21}$ box in Fig. 4 simply operates as an impedance inverter,[18] and no negative resistance is involved. Some thought on the matter will show that the response for a circuit like that in Fig. 20 which has three input resonators and three upper-sideband resonators will give a six-resonator filter response. Because of this property, it is advantageous to design the three resonators of the input filter in Fig. 20 as though they were the first three resonators of a six-resonator filter, and likewise for the three resonators of the upper-sideband filter.

To understand the basis for the procedure suggested above, consider the low-pass prototype with six reactive elements shown in Fig. 21(a). The ordinary Tchebycheff or maximally-flat prototypes of this sort having an even number of elements and one or more frequencies of perfect transmission are antimetric—*i.e.*, half the network is the dual of the other half. Because of this property such networks can always be put into the form shown in Fig. 21(b). The box marked K is an idealized impedance inverter which operates at all frequencies like a quarter-wavelength line of characteristic impedance K. Thus, (1) in Fig. 21 applies at all frequencies, where the size of K is specified by (2) in the figure. Note that the parameter α is available to adjust the impedance level of the right half of the network, and if α is chosen equal to one, the network in Fig. 21(b) will be symmetrical. In order to correspond to the resonator notation used in the preceding amplifier examples, we redesignate the elements on the left half of the modified circuit l_1, c_2, l_3, as shown in Fig. 21(b). The circuit on the left of Fig. 21(b) is then used as the prototype for both the input and the upper-sideband filter circuits.

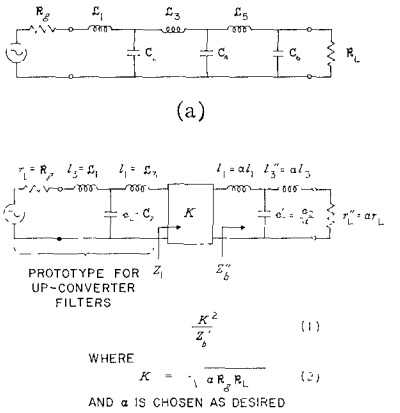

Fig. 21—Manner in which a three-reactive-element low-pass prototype for design of three input and three upper-sideband resonators of an up-converter is obtained from a six-reactive-element antimetric prototype.

It will be found that the approach described above can yield a much larger value of l_1 for the prototype than would be obtained if l_1 were taken as the end element of a complete, three-reactive-element prototype.[19] As in the preceding examples a larger value of l_1 will mean a larger bandwidth for the corresponding bandpass filters for the amplifier. Unfortunately, this same procedure will not work when f' is given by (4). In that case the imaginary part of Z_2 in Fig. 4 tends to have the same sign as the imaginary part of Z_b, while for this design procedure to work, the signs of the imaginary parts should be opposite so as to cause reactance cancellation. This happens when (60) and (61) apply.[20]

Ignoring R_s' in Fig. 4 and using (61) we obtain for $f=f_0$

$$(Z_2)_0 = \frac{(X_{12}X_{21})_0}{R_{b0}'} \tag{67}$$

[18] S. B. Cohn, "Direct-coupled-resonator filters," PROC. IRE, vol. 45, pp. 187–196; February, 1957.

[19] Examination of tables of prototype filter element values[8–10] shows that this statement holds for prototype filters having two times an odd number (but not two times an even number) of reactive elements.

[20] To verify these statements it is important to note that when (4) and (9) apply, if $f<f_0$, then $f'>f_0'$ and in Fig. 4 arg $Z_b \approx -\arg Z_b'$. When (60) applies, if $f<f_0$, then $f<f_0'$ and arg $Z_b \approx \arg Z_b'$. These facts along with (9) and (61) lead to the conclusions above.

where R_{b0}' is, as before, Z_b' evaluated at f_0'. Now $(Z_2)_0$ should equal $\mathfrak{R}_L$ shown in Fig. 21(a) scaled to the impedance level of R_{b0}. Thus

$$(Z_2)_0 = \frac{R_{b0}\mathfrak{R}_L}{\mathfrak{R}_g}. \tag{68}$$

Equating (67) and (68), and introducing the equal-bandwidth constraint given by (43), we obtain

$$R_{b0} = \sqrt{\frac{(X_{12}X_{21})_0}{\frac{\mathfrak{R}_L}{\mathfrak{R}_g}\left(\frac{f_0}{f_0'}\right)\left(\frac{x_1'}{x_1}\right)}} \tag{69a}$$

$$= a(X_{11})_0 \sqrt{\left(\frac{\mathfrak{R}_g}{\mathfrak{R}_L}\right)\left(\frac{x_1}{x_1'}\right)} \tag{69b}$$

and

$$R_{b0}' = R_{b0}\left(\frac{f_0}{f_0'}\right)\left(\frac{x_1'}{x_1}\right), \tag{70}$$

which establish the impedance levels of the input and upper-sideband filters. Then by (*b*) in Fig. 7 the fractional bandwidth of the input filter is

$$w = \frac{R_{b0}}{x_1}\left(\frac{\Omega_1 l_1}{r_L}\right) \tag{71a}$$

$$= \frac{a(X_{11})_0}{\sqrt{x_1 x_1'}} \sqrt{\frac{\mathfrak{R}_g}{\mathfrak{R}_L}\left(\frac{\Omega_1 l_1}{r_L}\right)}, \tag{71b}$$

and by (42) the fractional bandwidth of the output filter is

$$w' = \frac{w f_0}{f_0'}. \tag{72}$$

The design procedure may then be summarized as follows. First the f_0 and f_0' values must be selected to give adequate gain. In this case the idealized power gain ratio for any input frequency f and output frequency f' is given simply by f'/f; however, in a practical situation the actual gain will be less as a result of diode loss (and losses in the filters). An estimate of the actual midband gain can be obtained using the equation[5]

$$\left(\frac{W_L'}{W_s}\right)_0 = \left(\frac{f_0'}{f_0}\right)\frac{1}{(u + \sqrt{1+u^2})^2} \tag{73}$$

where

$$u = \frac{R_s}{\sqrt{(X_{12}X_{21})_0}} = \frac{1}{aQ_d}\sqrt{\frac{f_0'}{f_0}}. \tag{74}$$

Eqs. (73) and (74) give the maximum midband power gain possible for a given f_0'/f_0 and diode operating Q. As a result of the introduction of bandwidth considerations into the design process, the actual gain for an amplifier of maximum bandwidth will be a little less.

Having selected values for f_0 and f_0' which will yield adequate gain, the diode resonator circuit giving resonators X_1 and X_1' should be designed first so that resonator slope parameters x_1 and x_1' can be computed from the derivative expression in (b) of Fig. 7 evaluated at $\omega_0 = 2\pi f_0$ and $\omega_0' = 2\pi f_0'$, respectively. Then obtaining $\mathfrak{R}_g$ and $\mathfrak{R}_L$ from the unmodified form of the low-pass prototype shown in Fig. 21(a) and having values for $X_{12}X_{21}$ and f_0'/f_0, R_{b0} and R_{b0}' are computed by (69b) and (70). Then knowing Ω_1, r_L, and l_1 for the modified prototype shown in Fig. 21(b), w and w' can be computed by use of (71a) and (72). Having values for R_{b0}, w, R_{b0}', and w', the remaining resonator slope parameters for the input and upper-sideband filters are computed by use of (b) and (e) in Fig. 7, using the element values of the modified prototype filter shown in Fig. 21(b). The midband gain including diode loss can then be checked by use of (22), (23), and (66).

If the diode is resonated in shunt the procedure is essentially the same on the dual basis. The corresponding equations are

$$G_{b0} = a(B_{11})_0 \frac{f_0'}{f_0}\sqrt{\frac{\mathfrak{R}_g}{\mathfrak{R}_L}\frac{b_1}{b_1'}} \tag{75}$$

$$G_{b0}' = G_{b0}\frac{f_0}{f_0'}\frac{b_1'}{b_1} \tag{76}$$

$$w = \frac{a(B_{11})_0}{\sqrt{b_1 b_1'}}\frac{f_0'}{f_0}\sqrt{\frac{\mathfrak{R}_g}{\mathfrak{R}_L}\left(\frac{\Omega_1 l_1}{r_L}\right)}. \tag{77}$$

Eq. (72) applies as before, and the prototype is still defined as in Fig. 21. The extra f_0'/f_0 factor appearing in (75) and (77) but not in (69b) and (71b) occurs as a result of the fact that $(X_{12}X_{21})_0 = a^2(X_{11})_0^2(f_0/f_0')$ while $(B_{12}B_{21})_0 = a^2(B_{11})_0^2\,(f_0'/f_0)$.

XI. Examples of Wide-Band Up-Converters

A trial up-converter design was worked out assuming that $f_0 = 500$ Mc, $f_0' = 7600$ Mc, and that the normalized diode parameters are as indicated in Table II. As before, $(X_L)_0$ is the reactance of the parasitic inductance L_d in Fig. 20 at frequency f_0. Using the series transmission line parameters shown in the table, the diode is brought to resonance at f_0 with a slope parameter of $x_1 = 4.260$ and at frequency f_0' with a slope parameter of $x_1' = 24.670$. The filters were then designed from a six reactive element, 0.5-db Tchebycheff ripple, lumped-element prototype of the form shown in Fig. 21(a)[8–10] having the element values $\mathfrak{R}_g = 1.0000$, $\mathfrak{L}_1 = 1.7254$, $C_2 = 1.2479$, $\mathfrak{L}_3 = 2.6064$, $C_4 = 1.3137$, $\mathfrak{L}_5 = 2.4758$, $C_6 = 0.8696$, $\mathfrak{R}_L = 1.9840$, and the cutoff frequency $\Omega_1 = 1$. The element values for the converted form in Fig. 21(b) are $l_1 = 2.6064$, $c_2 = 1.2479$, $l_3 = 1.7254$, and $r_L = 1.000$. Carrying out the design as described in the preceding

TABLE II

NORMALIZED DESIGN PARAMETERS FOR DESIGNS NO. 9, 10, 11, AND 12
(Up-Converters of the Form in Fig. 20)

Design No. 9

Frequencies:

$f_0'/f_0=15.2125, \qquad f_p/f_0=14.2125$

For Diode:

$(X_{11})_0=3.700, \qquad a=C_1/C_0=0.25$
$(X_L)_0=0.03700, \qquad Q_d=1/(2\pi f_0 C_0{}^3 R_s)=120$

For Series Transmission Line:

$Z_0=5.180, \qquad f_R/f_0=2.5521$

Resonator Slope Parameters and Other Filter Parameters:

$x_1=4.260, \quad b_2=27.421, \quad x_3=2.820$
$x_1'=24.670, \quad b_2'=1095.6, \quad x_3'=16.333$

All unprimed resonators resonate at f_0 and all primed resonators resonate at f_0'

$R_{b0}=R_L=0.2727, \qquad R_{b0}'=R_L'=0.1038$

(The three-resonator input and output filter designs were derived from a six-reactive-element low-pass prototype with 0.5 db Tchebycheff ripple.)

Design No. 10

Same as Design No. 9 except that:

$b_2=x_3=b_2'=x_3'=0$
$R_{b0}=R_L=0.2355, \qquad R_{b0}'=R_L'=0.08968$

(The designs for the single-resonator input and output filters were derived from a two-reactive-element low-pass prototype with 1.0-db Tchebycheff ripple.)

Design No. 11

Same as Design No. 9 except that:

$b_2=x_3=b_2'=x_3'=0$
$R_{b0}=R_L=0.3877, \qquad R_{b0}'=R_L'=0.1478$

(The designs of the single-resonator input and output filters were worked out to give maximum gain at midband under the constraint that the input and output filters have the same bandwidth.)

Design No. 12

Same as Design No. 9 except that:

$b_2=x_3=b_2'=x_3'=0$
$R_{b0}=R_L=R_{b0}'=R_L'=0.2392$

(The designs of the single-resonator input and output filters were worked out in this case to give maximum mid-band gain regardless of bandwidth considerations.)

section, impedance levels and slope parameters as indicated for Design No. 9 in Table II are obtained. The fractional bandwidths of the input and upper-sideband filters are $w=0.1669$ and $w'=0.01097$.

The response of an amplifier of the form in Fig. 20 with the circuit parameters as indicated for Design No. 9 in Table II was computed using a digital computer and (64) and (65). The results are shown by the curve marked Design No. 9 in Fig. 22. With $f_0'/f_0=15.2$ the theoretical midband gain of a lossless amplifier would be 11.8 db. As is seen from the figure, the actual midband gain including the diode loss is about 10.2 db. If the diode had been lossless, a 0.5-db ripple, Tchebycheff response with six peaks and an equal-ripple bandwidth of 16.7 per cent would be expected. However, as a result of diode loss the band edges are rounded and the equal-ripple bandwidth is narrowed to about 14 per cent, though the 3-db bandwidth is still somewhat over 16 per cent.

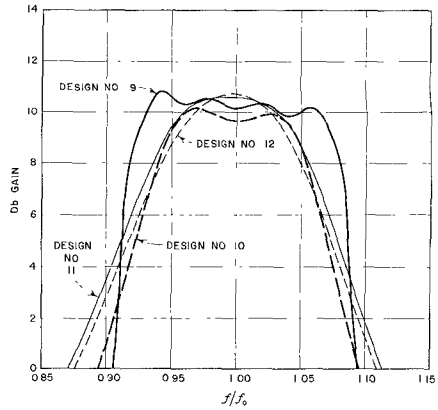

Fig. 22—The responses of some trial up-converter designs determined with a digital converter.

The curve marked Design No. 10 in Fig. 22 was computed using the corresponding parameters indicated in Table II. This design is for an analogous amplifier with a single input resonator and a single upper-sideband resonator with the design worked out from a two-reactive-element, 1.0-db ripple, Tchebycheff low-pass prototype. In this case a lossless amplifier should give an equal-ripple bandwidth of 10 per cent. As in the preceding example, the diode loss narrows the equal-ripple bandwidth and reduces the height of the ripples.

Design No. 11 in Table II and Fig. 22 was worked out so as to give maximum midband gain using single-resonator input and upper-sideband filters whose design was constrained by (43) so as to give equal input and upper-sideband filter bandwidths. Design No. 12 in Table II and Fig. 22 was worked out to give maximum midband gain regardless of any bandwidth considerations while using single-resonator input and upper-sideband filters.[5]

XII. NOISE FIGURE

The noise figure of several of the trial designs was computed assuming that the only degradation of the noise figure from the ideal is due to thermal noise in the diode loss resistance. On this basis Design No. 2 in Figs. 10 and 12 has a noise figure of 3.3 db when f is near f_0, as compared with an ideal noise figure of 3.0 db (as measured by the signal generator method[21]). Design No. 6 in Figs. 16 and 19 has a computed noise figure of 1.1 db (as measured by either the signal generator or noise source methods[21]), while Design No. 9 in Figs. 20 and 22 has a computed noise figure of 0.97 db. From these examples it is evident that design for maximum bandwidth (for given gain, etc.) is quite compatible with good noise figures.

[21] S. B. Cohn, "The noise figure muddle," *The Microwave J.*, vol. 2, pp. 7–11; March, 1959.

XIII. Conclusions

The use of lumped-element, low-pass prototype filters in the design of the band-pass filters for parametric amplifiers and up-converters is found to simplify the problem greatly. This is because once the lumped-element, low-pass prototype is specified, only the fractional bandwidths and impedance levels of the band-pass filters remain to be specified. Reducing the problem to this number of degrees of freedom is seen to make the design problem quite tractable. In the case of up-converters, ordinary lumped-element Tchebycheff or maximally-flat prototypes are found to be quite appropriate, but in the case of parametric amplifiers with the negative-resistance type of operation, such prototypes should be modified as indicated in Sections VI and VII in order to prevent high peaks of gain at the band edges. The two-reactive-element prototype given in the last paragraph of Section VII should be suitable for many cases where two-resonator filters are desired.

As can be seen from (37), (49) to (58), and (71b), the fractional bandwidths called for in the design of the band-pass filters of parametric amplifiers and up-converters are directly proportional to $a = C_1/C_0$. Further, it will be noted that in all of the equations in this paper the degradation of performance due to diode loss is always controlled by the parameter $(aQ_d) = (C_1/C_0)Q_d$ rather than by Q_d alone. [In the case of up-converters see (74).] Thus the size of C_1/C_0 is of vital importance in determining the bandwidth capabilities of a parametric amplifier or up-converter. At present little information is available as to the largest practical values that C_1/C_0 can take without overdriving the diode so as to degrade the noise figure. The value $a = C_1/C_0 = 0.25$ used in the examples of this paper is probably practical, though perhaps on the optimistic side.

In the case of degenerate parametric amplifiers the fractional bandwidth of the band-pass filter is *inversely* proportional to the resonator slope parameter x_1 (or b_1 for the diode resonated in shunt). For nondegenerate amplifiers and up-converters the fractional bandwidth w is inversely proportional to $\sqrt{x_1 x_1'}$ (or $\sqrt{b_1 b_1'}$ for the shunt resonance case). Thus it is of great importance to design the diode resonator circuit so as to minimize the reactance (or susceptance) slope at f_0 and f_0'. Stub tuners and the like must be avoided since they introduce unnecessary resonances and, as a result, large reactance slopes. If the diode resonator is a series resonator, it is desirable that it be followed immediately by a shunt resonator (or vice versa if the diode resonator is a shunt resonator). If the diode resonator and the next resonator of the filter are separated by a connecting line, part of the selectivity of the connecting line must be charged to the diode resonator, thus increasing the effective size of the diode resonator slope parameter and reducing the bandwidth which can be used in the filter.

In summary, the bandwidths which can be achieved in engineering practice will be influenced very much by the usable C_1/C_0 ratio of available diodes, and by the degree to which the slope parameters of the diode resonators can be minimized using practical circuitry. Though the examples presented herein involve a guess as to what C_1/C_0 should be and are idealized in some respects, they should be strongly suggestive of the performance that can be expected.

Correction

G. R. Valenzuela, author of "Impedances of an Elliptic Waveguide (For the ${}_eH_1$ Mode)," which appeared on pp. 431–435 of the July, 1960, issue of these Transactions, has brought the following to the attention of the *Editor*.

On page 433, read:

into Hz, and then integrating, it can be easily shown that

$$V = i\omega\mu \int_0^{u_0} \int_{-\pi/2}^{\pi/2} H_z(u, v)\, ds_1 ds_2 = 2 \int_0^{u_0} E_u\left(u, \frac{\pi}{2}\right) ds_1.$$

Also on page 433, pertaining to (4), read:

Now the impedances can be easily obtained. Let

$$Z_0 = 120\pi\left(\frac{\lambda g}{\lambda}\right) \quad \text{and} \quad h = q(k^2 - \beta^2)^{1/2},$$

then

$$Z_{WV} = \frac{h^4 {I_1}^2}{I_2} Z_0$$

and

$$Z_{WI} = \frac{I_2}{4{J_{e1}}^2(u_0)} Z_0. \tag{4}$$

On page 435, for (8) read:

The expression for the approximate impedances are

$$Z_{WV} = \frac{32}{3\pi} \frac{r(3 + r^2)}{(5 + 2r^2)} Z_0$$

$$Z_{WI} = \frac{3\pi}{32} \frac{r(15 + 11r^2 + 2r^4)}{(2 + r^2)^2} Z_0. \tag{8}$$